

The effect of rotational gravity darkening on magnetically torqued Be star discs

J. C. Brown,¹* D. Telfer,¹ Q. Li,^{1,2}* R. Hanuschik,³ J. P. Cassinelli⁴
and A. Kholtygin^{5,6}

¹*Department of Physics and Astronomy, University of Glasgow, Glasgow G12 8QQ*

²*Department of Astronomy, Beijing Normal University, Beijing 100875, China*

³*European Southern Observatory, Karl-Schwarzschild-Str. 2, 85748 Garching, Germany*

⁴*Department of Astronomy, University of Wisconsin–Madison, USA*

⁵*Astronomical Institute, St. Petersburg University, Saint Petersburg State University, V.V. Sobolev Astronomical Institute, 198504 Russia*

⁶*Isaac Newton Institute of Chile, St. Petersburg Branch*

Accepted 2004 May 6. Received 2004 April 27; in original form 2003 December 15

ABSTRACT

In the magnetically torqued disc (MTD) model for hot star discs, as proposed and formulated by Cassinelli et al., stellar wind mass loss was taken to be uniform over the stellar surface. Here account is taken of the fact that as the stellar spin rate $S_o (= \sqrt{\Omega_o^2 R^3 / GM})$ is increased, and the stellar equator is gravity darkened, the equatorial mass flux and terminal speed are reduced, compared with the poles, for a given total \dot{M} . As a result, the distribution of equatorial disc density, determined by the impact of northbound and southbound flows, is shifted further out from the star. This results, for high $S_o (\gtrsim 0.5)$, in a fall in the disc mass and emission measure, and hence in the observed emission line equivalent width, scattering polarization and infrared emission. Consequently, contrary to expectations, critical rotation $S_o \rightarrow 1$ is not the optimum for creation of hot star discs which, in terms of emission measure for example, is found to occur in a broad peak around $S_o \approx 0.5$ – 0.6 depending slightly on the wind velocity law.

The relationship of this analytic quasi-steady parametric MTD model to other work on magnetically guided winds is discussed. In particular, the failures of the MTD model for Be-star discs alleged by Owocki and ud-Doula are shown to revolve largely around open observational tests, rather than in the basic MTD physics, and around their use of insufficiently strong fields.

Key words: polarization – stars: emission-line, Be – stars: magnetic fields – stars: mass-loss – stars: rotation – stars: winds, outflows.

1 INTRODUCTION

Be stars are defined as ‘non-supergiant B-type stars whose spectra have, or had at one time, one or more Balmer lines in emission’ (Collins 1987). The pioneering research on Be stars by Struve proposed a rotational model with emission lines from equatorial discs (Struve 1931), but Be-star discs remain enigmatic despite many decades of detailed observations and research (Jaschek & Groth 1982; Slettebak 1982; Underhill & Doazan 1982; Slettebak & Snow 1987; Slettebak 1988; Smith, Henrichs & Fabregat 2000; Porter & Rivinius 2003). The main physics problems they pose are how the material in them (a) is delivered from the star, (b) becomes so dense, and (c) acquires such high angular momentum. The answer

to (a) undoubtedly lies in stellar radiation pressure. The first qualitative answer to (b) was the wind compressed disc (WCD) model of Bjorkman & Cassinelli (1993). In this, the angular momentum of rotating wind flow returns the matter to the equator where north and south streams collide and create a shock compressed disc. There are several snags with this model. First, it does not produce high enough densities. Second, the disc formed has mainly radial flows rather than the quasi-Keplerian azimuthal flows observed. Third, non-radial line-driving forces (Owocki, Cranmer & Gayley 1996) may cause polar rather than equatorial flow to dominate.

A phenomenological solution to these problems was proposed and quantified parametrically in the magnetically torqued disc (MTD) model of Cassinelli et al. (2002). This invokes a dipole-like field which steers the wind flow toward the equator and torques up its angular momentum on the way. The field torques up the wind flow to Keplerian speeds or higher and confines the radial flow redirecting it

*E-mail: john@astro.gla.ac.uk (JCB); li@astro.gla.ac.uk (QL)

to be poloidal and creating a shock compressed equatorial disc. The isothermal disc grows in thickness (but not in density) over comparatively long time-scales (\approx years) which are roughly consistent with long time-scale variability of some Be stars (Doazan 1982; Dachs 1987; Okazaki 1997; Telting 2000), allowing a quasi-steady treatment. There is growing observational evidence of reasonably strong fields (hundreds of gauss) in hot stars – e.g. ω Orionis with $B \sim 530 \pm 230$ G (Neiner et al. 2003), β Cephei with $B \sim 360 \pm 30$ G (Donati et al. 2001), θ^1 Orionis C with $B \sim 1100 \pm 100$ G (Donati et al. 2002), though some of these are very oblique and/or slow rotating and the MTD model is not directly applicable in its basic form.

In the MTD treatment the stellar wind mass flux and wind speed were taken to be uniform over the stellar surface. For the case of a rotating star, essential to creating a disc, this assumption is invalid. Rotation results in equatorial gravity darkening which reduces the wind mass flux and speed there, as described by Owocki, Gayley & Cranmer (1998). In this paper, we evaluate the effects of this on the MTD model. We do so by generalizing the basic quasi-steady parametric approach of MTD, but discussing in Section 5 issues concerning the properties of that description in relation to other theoretical and observational work on the problem. The MTD paper was really the first to model the combined effects of field and rotation but several earlier papers had discussed disc formation by magnetic channelling (Matt et al. 2000), while work subsequent to MTD has variously challenged it (Owocki & ud-Doula 2003), and supported it (Maheswaran 2003). Insofar as there remains a degree of disagreement in the literature over whether the model works for Be stars, our detailed results should be treated with some caution, though the general trends of the effect of gravity darkening should be sound.

2 EFFECT OF GRAVITY DARKENING ON DISC DENSITY

Owocki et al. (1998) showed that the mass flux from a stellar surface satisfies

$$F_{\text{mo}}(g) \propto g, \quad (1)$$

while the terminal speed satisfies

$$v_{\infty}(g) \propto g^{1/2}, \quad (2)$$

where g is the local effective gravity.

On a rotating sphere with stellar radius R and angular velocity Ω_0 , at colatitude θ , the net gravity is

$$\begin{aligned} g(\theta) &= \frac{GM}{R^2} - \frac{(\Omega_0 R \sin \theta)^2}{R \sin \theta} \sin \theta \\ &= \frac{GM}{R^2} - \Omega_0^2 R \sin^2 \theta \\ &= g_0 \left[1 - \frac{(\Omega_0 R)^2}{GM/R} \sin^2 \theta \right] \\ &= g_0 (1 - S_0^2 \sin^2 \theta), \end{aligned} \quad (3)$$

where $S_0 = \sqrt{\Omega_0^2 R^3 / GM}$ as in MTD. Strictly speaking, we should also include the effect of continuum scattering radiation pressure at least, which results in

$$g_0 = \frac{GM}{R^2} (1 - \Gamma_{\text{rad}}),$$

where $\Gamma_{\text{rad}} = L/L_{\text{Edd}}$ is the ratio of the stellar luminosity to the Eddington luminosity (Maeder & Meynet 2000).

It follows that the mass flux at θ becomes

$$F_{\text{mo}}(\theta) = K (1 - S_0^2 \sin^2 \theta), \quad (4)$$

where K is a constant, and the terminal speed for matter from θ is

$$v_{\infty}(\theta) = v_{\infty 0} (1 - S_0^2 \sin^2 \theta)^{1/2}, \quad (5)$$

where $v_{\infty 0}$ is the value of v_{∞} at $\theta = 0$.

Here we will assume the wind velocity obeys $v_w(r) = v_{\infty}(1 - R/r)^{\beta}$, but with

$$v_w(r, \theta) = v_{\infty}(\theta) \left(1 - \frac{R}{r} \right)^{\beta}, \quad (6)$$

where β is assumed not to depend on θ . This basically requires that wind acceleration occurs quite near the star and that the field lines are roughly radial there. We want to express K in terms of the total mass loss rate \dot{M}

$$\begin{aligned} \dot{M} &= \int_0^{\pi} F_{\text{mo}}(\theta) 2\pi R \sin \theta R d\theta \\ &= 4\pi R^2 K \int_0^{\pi/2} (1 - S_0^2 \sin^2 \theta) \sin \theta d\theta \\ &= 4\pi R^2 K \left(1 - \frac{2S_0^2}{3} \right). \end{aligned} \quad (7)$$

So by equation (4),

$$F_{\text{mo}}(\theta) = \frac{\dot{M}}{4\pi R^2 (1 - 2S_0^2/3)} (1 - S_0^2 \sin^2 \theta). \quad (8)$$

To relate this mass flux at θ on the stellar surface to that normal to the equatorial plane at distance $x = r/R$, we follow Cassinelli et al. (2002) in parametrizing the decline of the magnetic field, B , with equatorial plane distance according to

$$B(x) = B_0 x^{-b}, \quad (9)$$

where B_0 is taken as uniform over, and normal to, the stellar surface, and b is a constant with a dipole field $b = 3$. Flux conservation then requires that the cross-sectional area dA of a flux tube arriving at the equator is related to its area dA_0 at the star by $B dA = B_0 dA_0$ or

$$dA(x) = dA_0 x^b. \quad (10)$$

However, $dA(x) = 2\pi R^2 x dx$ and $dA_0 = 2\pi R^2 \sin \theta d\theta$ so that the relation between θ and x is given by integrating $\sin \theta d\theta = x^{-b+1} dx$, to yield

$$\cos \theta = C - \frac{x^{-b+2}}{b-2}. \quad (11)$$

Requiring that $x \rightarrow \infty$ for $\theta \rightarrow 0$ implies $C = 1$ so that

$$\cos \theta(x) = 1 - \frac{x^{-b+2}}{b-2}. \quad (12)$$

For the particular case $b = 3$ (the dipole case) mainly discussed by Cassinelli et al. (2002), and which we focus on henceforth, this yields

$$\cos \theta(x) = 1 - \frac{1}{x}. \quad (13)$$

We can now obtain the mass flux $F_m(x)$ at x near the equatorial plane by using $F_m(x) = F_{\text{mo}}(\theta) dA_0(\theta)/dA(x)$ and using equations (8),

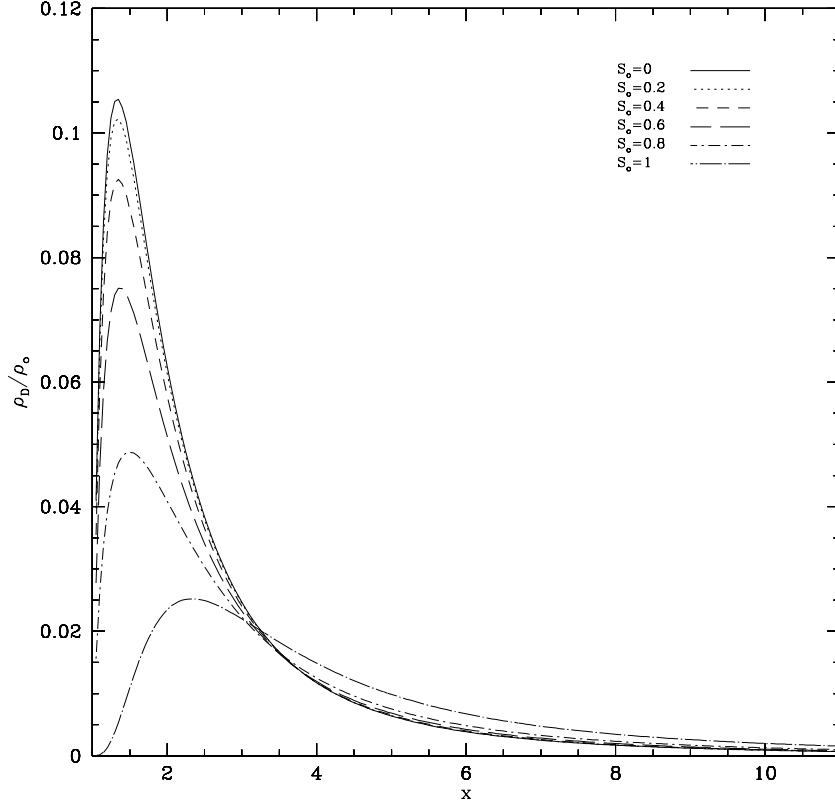


Figure 1. Disc density ρ_D/ρ_0 versus equatorial distance x for various spin rates, S_0 . Disc density increases rapidly then decreases sharply again. The peak value decreases and moves out as S_0 increases, but the peak is in the range $x \approx 1.3\text{--}2.3$ for all S_0 .

(10) and (13), namely

$$F_m(x) = \frac{\dot{M}}{4\pi R^2 (1 - 2S_0^2/3)} x^{-3} \times \left\{ 1 - S_0^2 \left[1 - \left(1 - \frac{1}{x} \right)^2 \right] \right\}, \quad (14)$$

while by equations (5), (6) and (13), the wind speed there is

$$v_w(x) = v_{\infty 0} \left(1 - \frac{1}{x} \right)^\beta \left\{ 1 - S_0^2 \left[1 - \left(1 - \frac{1}{x} \right)^2 \right] \right\}^{1/2}, \quad (15)$$

and the arriving wind ram pressure $P_{\text{ram}}(x) = F_m(x)v_w$ is

$$P_{\text{ram}} = \frac{\dot{M} v_{\infty 0}}{4\pi R^2} x^{-3} \left(1 - \frac{1}{x} \right)^\beta \frac{\left\{ 1 - S_0^2 \left[1 - \left(1 - \frac{1}{x} \right)^2 \right] \right\}^{3/2}}{1 - 2S_0^2/3}. \quad (16)$$

The high density $\rho_D(x)$ of the cool, shock-compressed, disc (WCD) in the equatorial plane is then given as in the WCD model (and in MTD) by the isothermal disc (sound speed c_s) pressure balance expression $\rho_D c_s^2 = P_{\text{ram}} = P_D$ or by equation (16)

$$\rho_D(S_0, x) = \rho_0 x^{-3} \left(1 - \frac{1}{x} \right)^\beta \frac{\left\{ 1 - S_0^2 \left[1 - \left(1 - \frac{1}{x} \right)^2 \right] \right\}^{3/2}}{1 - 2S_0^2/3}. \quad (17)$$

Here

$$\rho_0 = \frac{\dot{M}}{4\pi R^2 v_{\infty 0}} \left(\frac{v_{\infty 0}}{c_s} \right)^2 \quad (18)$$

which is equivalent to ρ_{Dc} in the MTD model. Based on equation (17), we can write the disc density allowing for rotational grav-

ity darkening, compared to that neglecting it (e.g. MTD) as

$$\Psi(S_0, x) = \frac{\rho_D(S_0, x)}{\rho_D(0, x)} = \frac{\left[1 - \frac{S_0^2}{x} \left(2 - \frac{1}{x} \right) \right]^{3/2}}{1 - 2S_0^2/3} \quad (19)$$

with the property $\Psi(S_0, 1) = (1 - S_0^2)^{3/2}/(1 - 2S_0^2/3)$ which is < 1 for all S_0 , and tends to 0 as $S_0 \rightarrow 1$. This is because the equatorial wind flow falls with increasing S_0 , reducing the inner disc compression. On the other hand, if we (formally – see the comments below in Section 3) apply equation (19) as $x \rightarrow \infty$ we would get for the disc behaviour

$$\Psi(S_0, \infty) \rightarrow \frac{1}{1 - 2S_0^2/3}. \quad (20)$$

This is always > 1 because the polar wind supply of mass to large, equatorial distances x , is increased (for fixed \dot{M}) for large S_0 . Also, as $S_0 \rightarrow 1$ (critical rotation) we find

$$\Psi(1, x) = 3 \left(1 - \frac{1}{x} \right)^3 \quad (21)$$

which is > 1 at $x > 3^{1/3}/(3^{1/3} - 1) \approx 3.26$. In Figs 1 and 2, we show ρ_D/ρ_0 and $\Psi(S_0, x)$ versus x for various S_0 . Fig. 1 shows the disc density peaks in the range $x \approx 1.3 - 2.3$ for all S_0 , then to decrease rapidly with x for all S_0 .

3 EFFECT OF GRAVITY DARKENING ON DISC EXTENT, MASS AND EMISSION MEASURE

We have seen that $\rho_D(x)$ decreases and moves its maximum somewhat to larger x values as S_0 increases. However, we need also to

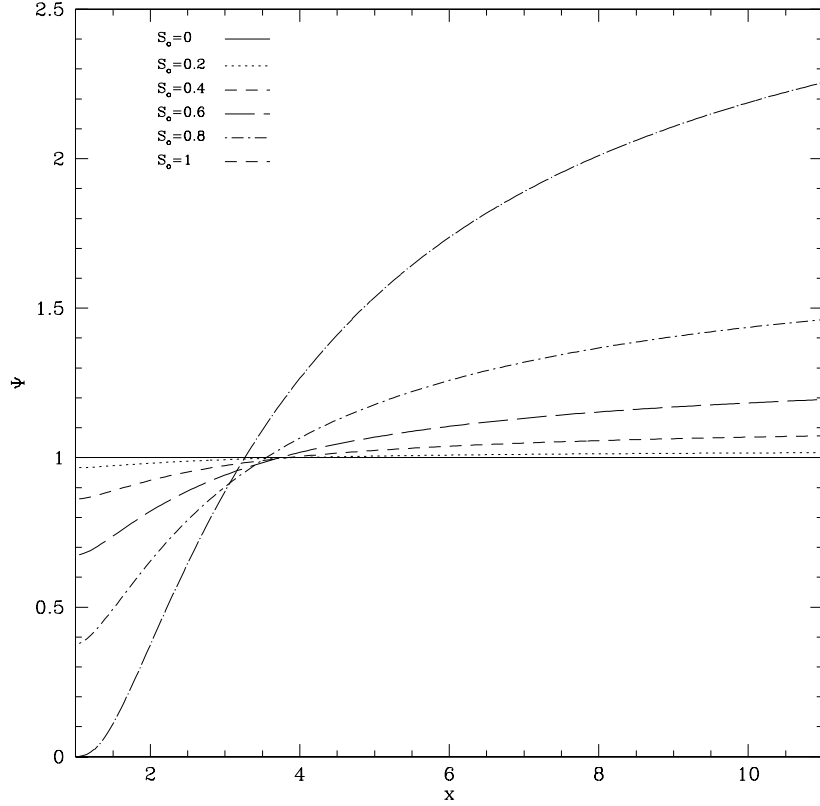


Figure 2. Ratio of disc density to that without gravity darkening $\Psi = \rho_D(S_0, x)/\rho_D(0, x)$ versus equatorial distance x for various spin rates S_0 .

consider the extent of the disc, i.e. the lower and upper boundaries of equation (17) in x as limited by the magnetic field strength. While enhancement of ρ_D locally enhances the local contribution per unit volume ($\sim \rho_D^2$) to the disc emission measure, it makes the material there harder to torque so that the extent of the disc is modified. In particular, for example, equation (20) is not valid in practice since the rapid decline in $B(x)$, as x goes up, limits the torquing to a finite distance.

To estimate the effect of including rotational gravity darkening on observable disc properties, we need to assess the effect on the inner and outer disc boundaries. Here we do so using a somewhat simpler treatment than that in MTD, namely what MTD termed the ‘switch approximation’. In this, the disc is taken to be rigidly torqued by the magnetic field (i.e. $v = v_0 x$, where $v_0 = S_0 \sqrt{GM/R}$) out to the distance where the magnetic energy density $B^2/8\pi$ falls below the rotational kinetic energy density $U_{KE} = \frac{1}{2}\rho_D v^2$. We have then, by equation (9),

$$U_B = \frac{B^2}{8\pi} = \frac{B_0^2}{8\pi} x^{-6} \quad (22)$$

and by equation (17)

$$U_{KE} = \frac{1}{2}\rho_0 \frac{GM}{R} S_0^2 x^{-1} \left(1 - \frac{1}{x}\right)^\beta \times \frac{\left\{1 - S_0^2 \left[1 - \left(1 - \frac{1}{x}\right)^2\right]\right\}^{3/2}}{1 - 2S_0^2/3}. \quad (23)$$

So the outer disc boundary $x = x_{\text{outer}}(S_0, \gamma)$ is given by setting $U_B = U_{KE}$. Thus x_{outer} is the solution x to

$$x^5 \left(1 - \frac{1}{x}\right)^\beta \frac{\left\{1 - S_0^2 \left[1 - \left(1 - \frac{1}{x}\right)^2\right]\right\}^{3/2}}{1 - 2S_0^2/3} = \frac{\gamma^2}{S_0^2}, \quad (24)$$

where

$$\gamma = \left(\frac{B_0^2/8\pi}{GM\rho_0/2R}\right)^{1/2} \quad (25)$$

is a measure of field energy compared to the disc gravitational energy. The inner disc boundary in the present approximation is simply the Keplerian rotation distance (cf. MTD)

$$x_{\text{inner}} = S_0^{-2/3}. \quad (26)$$

4 RESULTS AND DISCUSSION

In Figs 3 and 4, we show $x_{\text{inner}}(S_0)$ and $x_{\text{outer}}(S_0)$ versus S_0 for various γ values, and the corresponding colatitudes, on the stellar surface, of x_{inner} and x_{outer} in terms of equation (13). It turns out that these boundaries do not change greatly with S_0 once S_0 is larger than 0.2–0.3, but change a lot with γ , and that the mass flux reaching the disc comes from a rather small range of colatitudes (e.g. for $S_0 = 0.6$, $45^\circ \lesssim \theta \lesssim 70^\circ$ with $\gamma = 6$ – see Fig. 4). Mass flow from the pole (small θ) leaves the star as part of the wind while equatorial flow (large θ) does not achieve Keplerian speed.

According to equation (25), γ is determined by the magnetic and gravitational fields. In order to make mass-flux channelling and torquing possible, γ has to be substantially greater than unity. In terms of observations, the magnetic fields of Be stars are no larger than hundreds of gauss. Hence, γ should probably be in the range of 1–10 for Be stars to meet this requirement. In Figs 3 and 4, we also

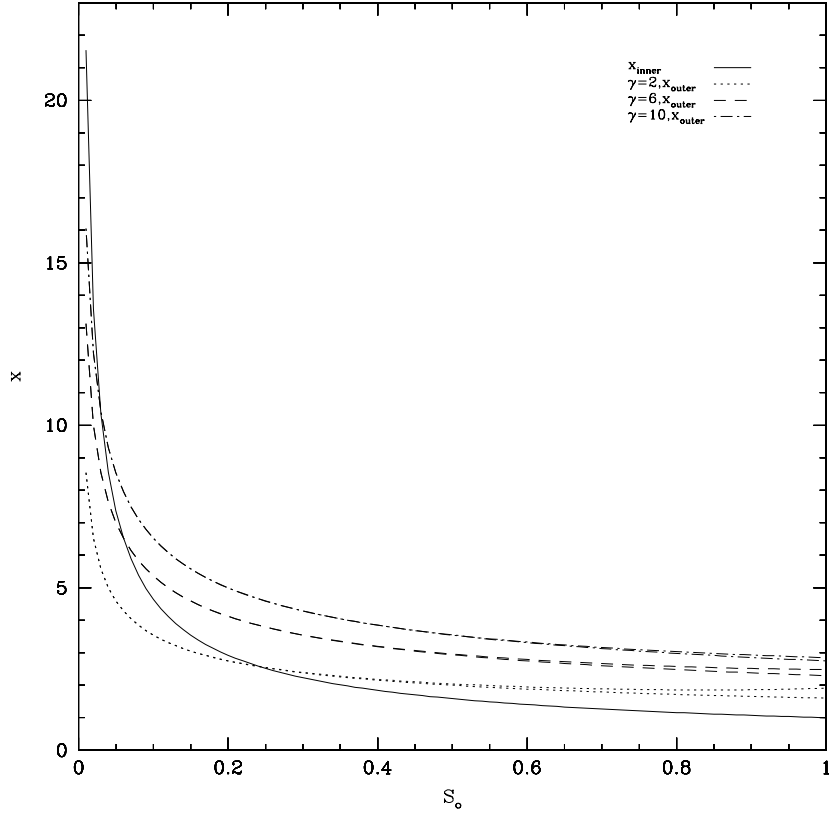


Figure 3. Disc boundaries x_{inner} and x_{outer} versus S_0 for various γ . The solid line corresponds to the inner radius x_{inner} , and the other lines to the outer radius of the disc for various γ . Each pair of curves with the same line type gives results with gravity darkening (upper curve) and without gravity darkening (lower curve). For larger γ , one requires smaller S_0 in order for a disc to form ($x_{\text{outer}} > x_{\text{inner}}$). This implies that for small magnetic fields, a relatively fast spin rate S_0 is necessary, while for large magnetic fields, moderate S_0 is adequate. Comparing curves with and without gravity darkening shows that gravity darkening has only a minor effect on the outer radius of the disc for any given γ , S_0 .

see that for smaller γ , a larger S_0 is necessary for a disc (clearly, the outer radius of the disc must be larger than the inner radius). These two figures also show that the gravity darkening has a small effect on the outer radius of the disc, which is within $\sim 5R$ for appropriate γ and S_0 . Similar outer boundaries have been derived for some stars using different disc models by Dougherty et al. (1994) and Coté, Waters & Marlborough (1996).

The detection of discs by polarization, infrared emission, and emission line strength is related to their mass and their emission measure which are proportional to $\int_V \rho_D dV$ and $\int_V \rho_D^2 dV$, respectively, where V is the disc volume. If the disc has thickness $H(x) = h(x)R$ at distance x then it contains a total number of particles

$$N = \frac{2\pi R^3}{m} \int_{x_{\text{inner}}(S_0)}^{x_{\text{outer}}(S_0, \gamma)} \rho_D(x) h(x) x dx, \quad (27)$$

and has emission measure

$$\text{EM} = \frac{2\pi R^3}{m^2} \int_{x_{\text{inner}}(S_0)}^{x_{\text{outer}}(S_0, \gamma)} \rho_D^2(x) h(x) x dx, \quad (28)$$

where m is the mean mass per particle. Using equation (17) these yield

$$N = N_0 \int_{x_{\text{inner}}(S_0)}^{x_{\text{outer}}(S_0, \gamma)} \frac{x^{-2} h(x)}{1 - 2S_0^2/3} \left(1 - \frac{1}{x}\right)^\beta \times \left\{ 1 - S_0^2 \left[1 - \left(1 - \frac{1}{x}\right)^2 \right] \right\}^{3/2} dx, \quad (29)$$

where $N_0 = 2\pi R^3 \rho_0/m$, and

$$\text{EM} = \text{EM}_0 \int_{x_{\text{inner}}(S_0)}^{x_{\text{outer}}(S_0, \gamma)} \frac{x^{-5} h(x)}{(1 - 2S_0^2/3)^2} \left(1 - \frac{1}{x}\right)^{2\beta} \times \left\{ 1 - S_0^2 \left[1 - \left(1 - \frac{1}{x}\right)^2 \right] \right\}^3 dx, \quad (30)$$

where $\text{EM}_0 = 2\pi R^3 (\rho_0/m)^2$.

Following the Brown & McLean (1977) formulation, the scattering polarization is $P = \tau(1 - 3\Gamma) \sin^2 i$, where τ is the optical depth, Γ is the shape factor of the disc and i is the inclination angle. Assuming the disc to be a slab with constant thickness $H = Rh$ and including the finite source depolarization factor $D = \sqrt{1 - R^2/r^2} = \sqrt{1 - 1/x^2}$ (Cassinelli, Nordsieck & Murison 1987; Brown, Carlaw & Cassinelli 1989), then we have the optical depth τ ,

$$\tau = \frac{3\sigma_T}{16} \int_{r_1}^{r_2} \int_{\mu_1}^{\mu_2} n(r, \mu) D(r) dr d\mu = \frac{3\sigma_T R}{16} \int_{x_{\text{inner}}}^{x_{\text{outer}}} \int_0^h n(x, z) D(x) \frac{x}{x^2 + z^2} dx dz = \tau_0 \int_{x_{\text{inner}}}^{x_{\text{outer}}} x^{-3} \left(1 - \frac{1}{x}\right)^\beta \frac{[1 - S_0^2 (\frac{2}{x} - \frac{1}{x^2})]^{3/2}}{1 - 2S_0^2/3} \times \sqrt{1 - \frac{1}{x^2}} \arctan \frac{h}{x} dx, \quad (31)$$

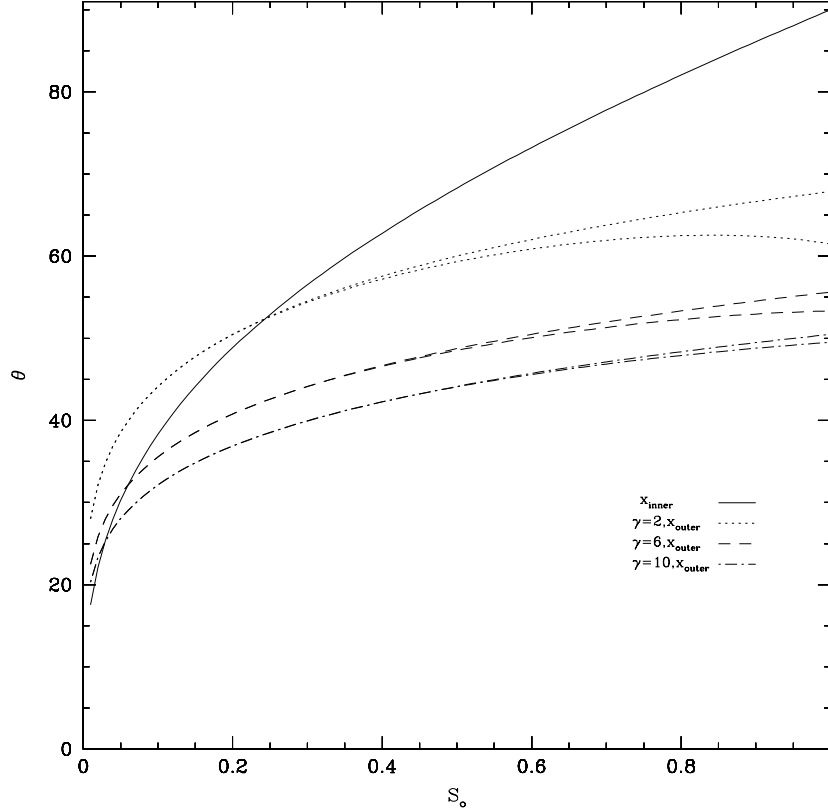


Figure 4. Stellar surface colatitudes θ° corresponding to the inner and outer disc boundaries, versus S_0 for various γ . The solid line corresponds to the inner boundary, and the other lines to outer boundaries of the disc. Each pair of curves with the same line type gives results with gravity darkening (lower curve) and without gravity darkening (upper curve). The possible range of colatitudes channelling matter are angles between the curve of solid-line type and the other curve for a given γ .

where

$$\tau_o = \frac{3\sigma_T R \rho_o}{16 m},$$

σ_T is the Thomson cross-section, $n = \rho_D/m$ is the electron density of the disc, and μ is the cosine of the angles between the incident light to the disc and the rotational axis. As in MTD, we neglect the absorption and suppose a fully ionized disc. The shape factor Γ yields

$$\begin{aligned} \Gamma &= \frac{\int_{r_1}^{r_2} \int_{\mu_1}^{\mu_2} n(r, \mu) D(r) \mu^2 dr d\mu}{\int_{r_1}^{r_2} \int_{\mu_1}^{\mu_2} n(r, \mu) D(r) dr d\mu} \\ &= \frac{\int_{x_{\text{inner}}}^{x_{\text{outer}}} n(x) D(x) \left[\frac{1}{2x} \arctan \frac{h}{x} - \frac{h}{2(h^2+x^2)} \right] x dx}{\int_{x_{\text{inner}}}^{x_{\text{outer}}} n(x) D(x) \arctan \frac{h}{x} dx}. \end{aligned} \quad (32)$$

Substituting equations (31) and (32) in the original polarization expression and after some reduction, yields the polarization, P , with gravity darkening effects,

$$P = P_o I_p \quad (33)$$

where

$$P_o = \tau_o = \frac{3\sigma_T R \rho_o}{16m}$$

and I_p is the integral

$$\begin{aligned} I_p &= \int_{x_{\text{inner}}}^{x_{\text{outer}}} x^{-3} \left(1 - \frac{1}{x} \right)^\beta \frac{[1 - S_o^2 \left(\frac{2}{x} - \frac{1}{x^2} \right)]^{3/2}}{1 - 2S_o^2/3} \\ &\quad \times \sqrt{1 - \frac{1}{x^2}} \arctan \frac{h}{x} dx (1 - 3\Gamma) \sin^2 i. \end{aligned} \quad (34)$$

Then $I_p = P/P_o$ is found numerically and shown in Figs 7 and 11 below for $h = 0.5$ with respect to typical half-opening angles of the disc about 10° (e.g. Hanuschik 1996; Porter 1996), and the inclination angle $i = 90^\circ$.

In Figs 5 and 6, we show the results of equations (29) and (30) for $N(S_o, \gamma)$ and $EM(S_o, \gamma)$ together with those obtained when gravity darkening is ignored (using the same switch approximation). For the latter, we use the integrands as in equations (29) and (30), but with $S_o = 0$; the same lower limit $x_{\text{inner}} = S_o^{-2/3}$ as given by equation (26), and the outer limit the solution to equation (24), with $S_o = 0$ on the left. We see that increasing S_o from zero results in a rising disc mass and emission measure up to a broad maximum at $S_o \lesssim 0.5$ and falling back almost to 0 as $S_o \rightarrow 1$. It is not surprising to see that gravity darkening has strong effects on the total number of particles and emission measure, since gravity darkening effects significantly reduce the mass flow from equatorial stellar regions into the disc. We also note that N/N_o and EM/EM_o ratios have peaks at about $S_o \approx 0.5$ for all γ , while for no gravity darkening they essentially keep increasing. Similar results are shown in Fig. 7 for the polarization which depends mainly on the disc electron scattering mass. The higher the total number of particles in the disc, the stronger the polarization. If gravity darkening were neglected, one would get a large I_p so a small P_o , for a given observed polarization value P (equation 33). This would imply a smaller ρ_o since $P_o \propto \rho_o$, which implies an underestimation of the mass-loss rate \dot{M} (equation 18), if we ignore gravity darkening.

The previous treatment is for fixed $\beta = 1$. In order to see the influence of the velocity law on the results, we tried various β values for a given γ . Fig. 8 shows that a wind velocity law has minor effects

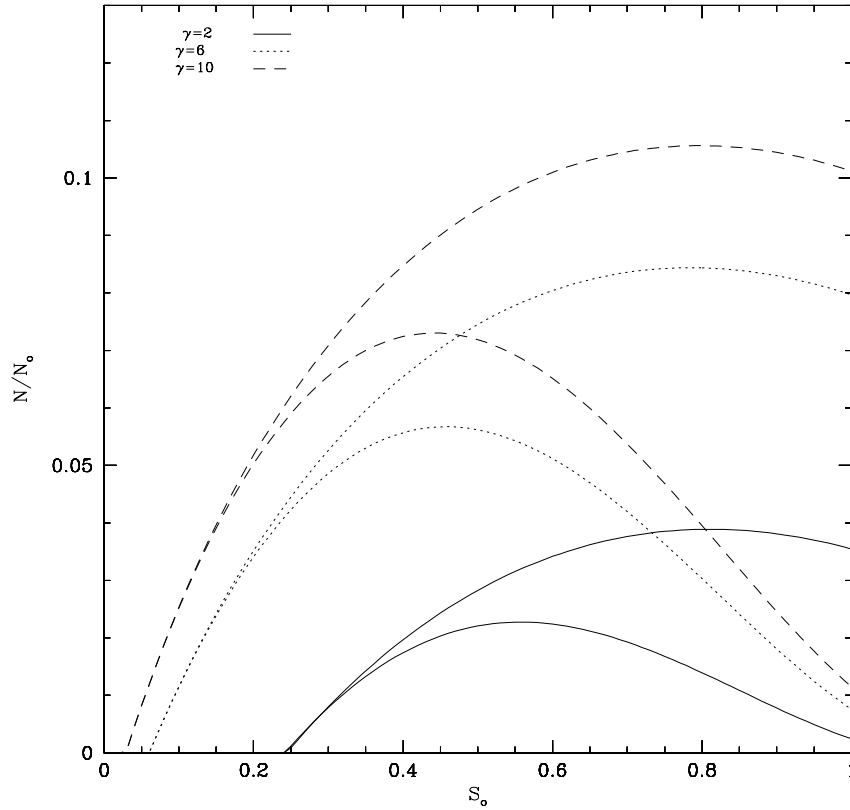


Figure 5. Ratio of total number of particles in the disc N/N_0 relative to an arbitrary reference value N_0 , versus S_0 for various γ . Lower and upper curves with the same line type are for gravity darkening and no gravity darkening, respectively. Gravity darkening significantly decreases the results as S_0 becomes large, and produces a peak. For larger γ , a smaller S_0 gives rise to the formation of a disc, so the curve becomes wider. The larger γ , the bigger N/N_0 .

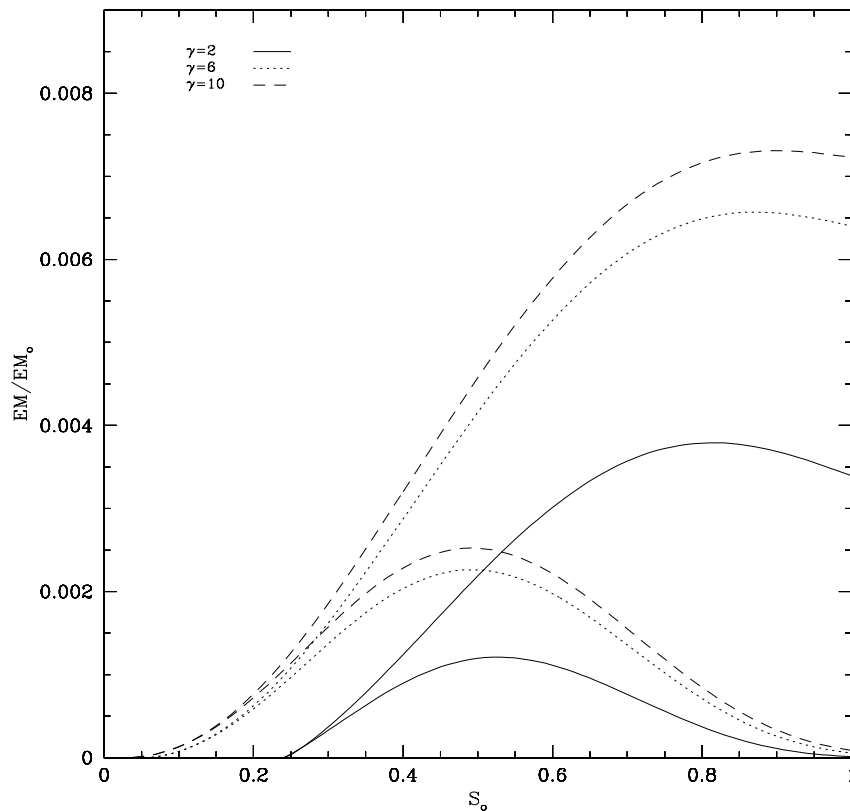


Figure 6. Ratio of emission measure EM/EM_0 relative to an arbitrary reference value EM_0 , versus S_0 for various γ . Lower and upper curves with the same line type are for gravity darkening and no gravity darkening, respectively.

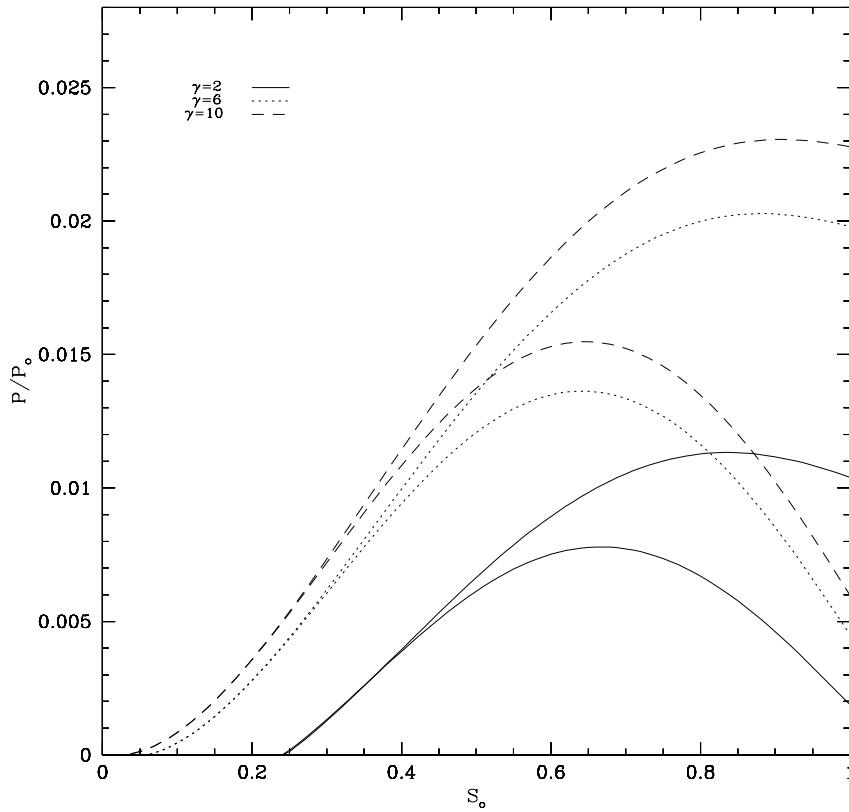


Figure 7. Ratio of polarization P/P_0 relative to an arbitrary reference value P_0 , versus S_0 for various γ . The inclination angle is assumed to be 90° (edge-on observation). Lower and upper curves with the same line type are for gravity darkening and no gravity darkening, respectively.

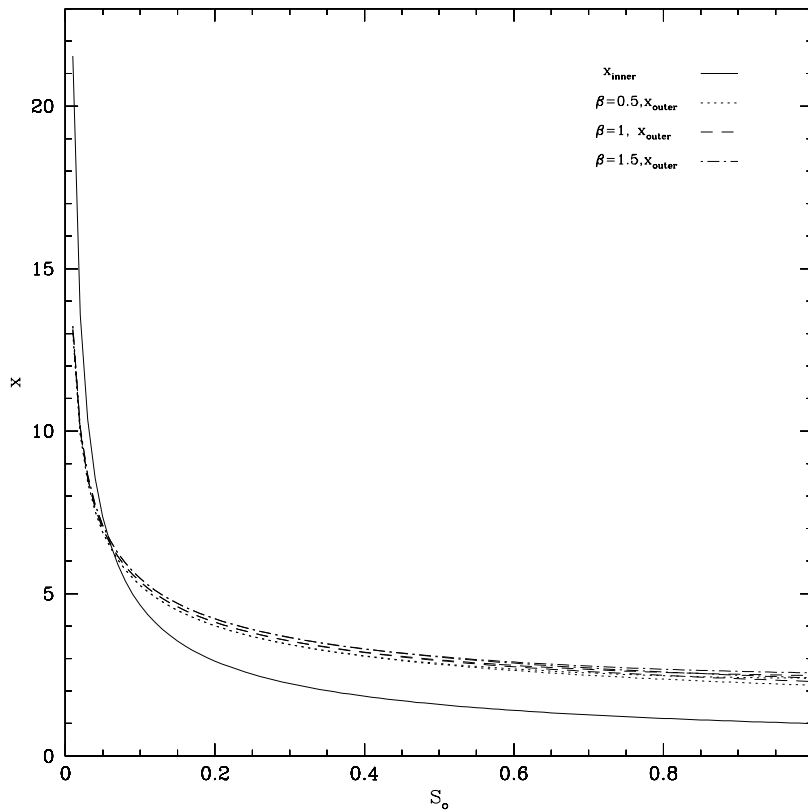


Figure 8. Disc boundaries x_{inner} and x_{outer} versus S_0 for various β with $\gamma = 6$. The solid line corresponds to the inner boundary x_{inner} , and the other lines to outer boundaries of the disc. Lower and upper curves of the same line type are for gravity darkening and no gravity darkening, respectively.

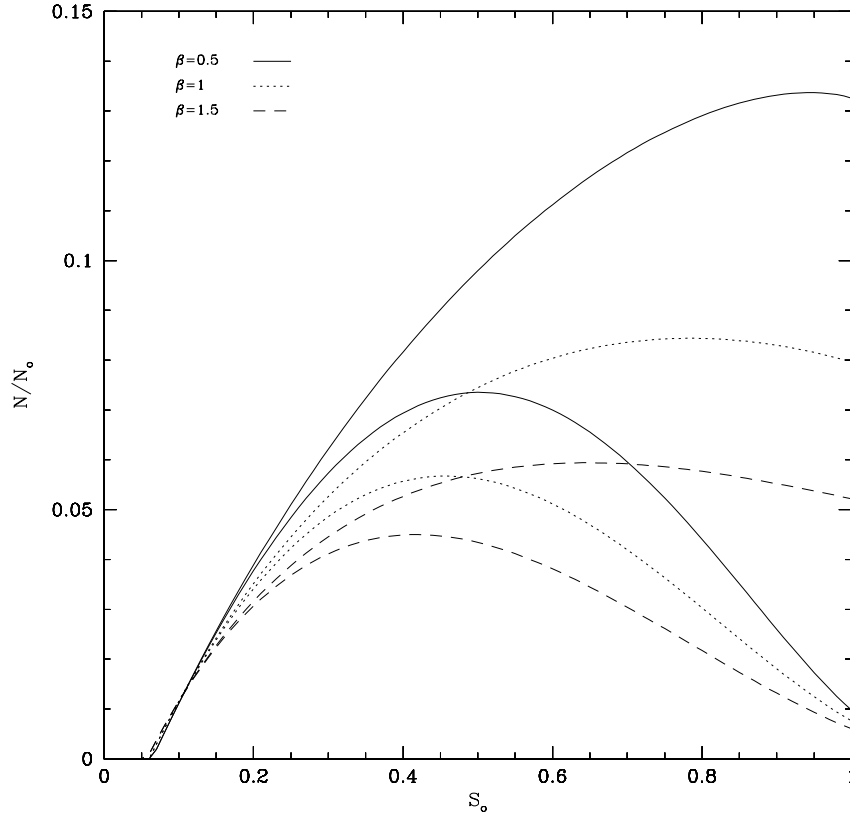


Figure 9. Ratio of total number of particles N/N_0 relative to an arbitrary reference value N_0 , versus S_0 for various β with $\gamma = 6$. Lower and upper curves of the same line type are for gravity darkening and no gravity darkening, respectively.

on the disc boundaries and so does gravity darkening. Figs 9–11 show that slower winds (i.e. bigger β values) will lead to a much smaller total number of particles, emission measure and polarization of the disc, as well as gravity darkening, significantly decreases these disc properties. From the plots we see that, for small $\beta = 0.5$, the total number of particles, emission measure and polarization peaks shift slightly to larger rotation rate ($S_0 \approx 0.6$), while a statistical study of observation data indicates the most common $S_0 \approx 0.7$ (Porter 1996) which, in our interpretation, would favour small β , i.e. fairly fast acceleration of winds from the stellar surface. If individual disc detectability peaks for $S_0 \approx 0.6$ and actual detection peaks for $S_0 \approx 0.7$, either there is a bias/selection effect in operation (Townsend, Owocki & Howarth 2004), or there is an upward trend in the frequency distribution of S_0 values.

5 COMPARISON OF MTD WITH MHD SIMULATIONS AND OTHER WORK ON MAGNETIC CHANNELLING

It was noted in Section 1 that the MTD model is phenomenological and parametric, and not a full solution to the physics equations. It is aimed, like all such models, at describing the main features of a system accurately enough to reproduce the essential physics but simple enough to facilitate ready incorporation of additional effects (such as gravity darkening) and comparisons with data. It is of course important to evaluate how well the MTD model describes reality when compared with more complete solutions. A full and detailed comparison is beyond the scope of this paper but we summarize here the present status as we see it of the relation of MTD to recent analytic and numerical work on closely related problems.

One of the earliest studies of the problem which found disc formation was that in a ‘magnetospheric’ context examined by Havnes & Goertz (1984). Keppens & Goedbloed (1999, 2000) carried out numerical simulations of magnetized stellar winds with rather weak fields and found disc ‘stagnation zones’ in the equatorial plane. Matt et al. (2000) studied non-rotating winds in dipole fields and found persistent equatorial disc structures around asymptotic giant branch (AGB) stars though with a steady throughput of mass leaking through the disc. Maheswaran (2003) conducted a detailed analytic study of the MTD situation and found that persistent discs are formed for quite small fields though he obtained somewhat tighter field constraints than MTD on the relevant regimes of magnetic field and spin rate. In the magnetohydrodynamic (MHD) simulations of isothermal flow driven outward from a non-rotating star with dipole magnetic fields, ud-Doula & Owocki (2002) found that the effect of magnetic fields in channelling stellar winds depends on the overall ratio of magnetic to flow kinetic energy density (as did MTD) and obtained disc results with rather low fields.

In contrast to all of these, in the ud-Doula & Owocki (2003) conference paper, based on the same code as ud-Doula & Owocki (2002), the interpretation shifts somewhat and seems more negative about disc persistence. Owocki & ud-Doula (2003) added rotation to their earlier work and concluded that no stable disc could form, with matter either falling back or bursting out after a modest number of flow times. In fact, the MHD code they used is incapable of handling the larger fields which MTD argued were required and which are recently in fact observed (several hundred gauss) in some Be stars, so their numerical results are not that relevant. Furthermore, given that observed fields are strong enough so that the wind is bound to be steered and torqued to the equatorial regions, if the behaviour

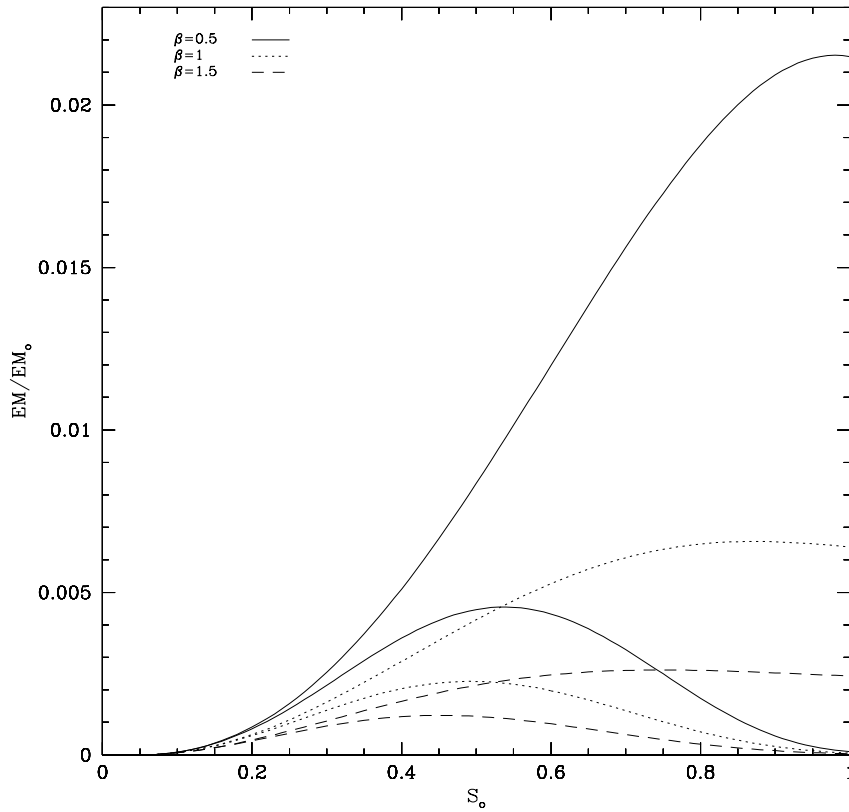


Figure 10. Ratio of emission measure EM/EM_0 relative to an arbitrary reference value EM_0 , versus S_0 for various β with $\gamma = 6$. Lower and upper curves of the same line type are for gravity darkening and no gravity darkening, respectively.

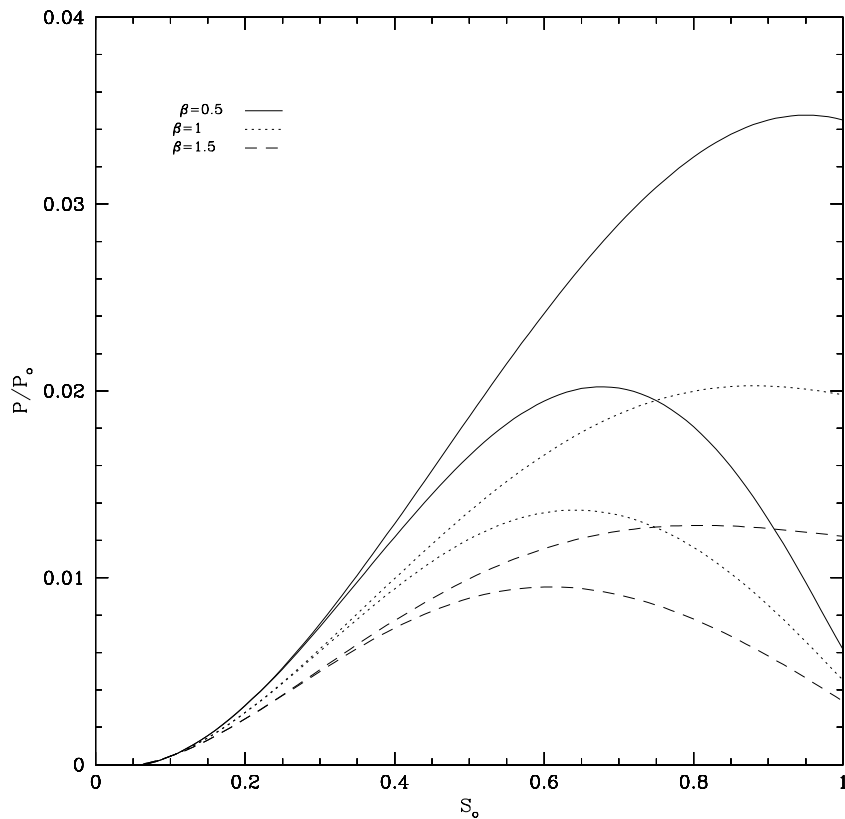


Figure 11. Ratio of polarization P/P_0 relative to an arbitrary reference value P_0 , versus S_0 for various β with $\gamma = 6$. The inclination angle is assumed to be 90° (edge-on observation). Lower and upper curves of the same line type are for gravity darkening and no gravity darkening, respectively.

of that matter were highly unstable as in simulation results of ud-Doula and Owocki, we should observe very frequent Be star disc disruption, which we do not. In fact we see no reason why material should fall back, given that it is centrifugally supported, until the dipole structure fills up. This takes a very large number of flow times (many years) – hence the quasi-steady formulation in MTD. In the case of weak fields and low rotation, fall back and burst out of matter is not altogether surprising, but it is not clear why the Owocki & ud-Doula (2003) simulation results conflict with those of others. For stronger fields using order-of-magnitude scaling estimates, they found that discs, essentially like MTD, can form and have gone on to develop scenarios for strong fields closely akin to MTD under the names magnetically rigid disc and magnetically confined wind-shocked disc. They were, however, dismissive of the relevance of this to Be-stars. This was not on the grounds of the physics of MTD but over the issue of whether a semirigid disc near corotation can be reconciled with observations of Be-stars, specifically spectrum line shapes and the long-term violet-to-red (V/R) variations. The work of Telfer et al. (2003) suggests that the former is not a serious problem. The issue of the V/R variations was emphasized in the original MTD paper which recognized that, if MTD is the correct description of Be disc formation, a close examination is required of how the V/R variations could arise. At first sight it would seem that the conventional interpretation in terms of spiral density waves (induced by the non-spherical potential) in a Keplerian disc would not work if the field controlled the disc, and another interpretation would have to be found but it depends on the rate of viscous diffusive redistribution of disc matter toward Keplerian (Maheswaran 2003). Until further testing is carried out we are therefore of the view that the MTD model remains a good basic scheme for further modelling work. We also note that, when MTD is applied across the range of hot star spectral types, it offers a remarkably good explanation of the narrow spectral range where discs are in fact detected. No other model offers any explanation of this observation.

6 CONCLUSIONS

We have discussed the phenomenological magnetically torqued disc model of Cassinelli et al. (2002) for hot (particularly Be) star disc formation in relation to other work on magnetically steered wind creation of disc like structures, concluding that, for moderate fields comparable to those observed, the description is physically realistic but that further work is needed to see if its disc velocity structure can be reconciled with observations including line profiles and V/R variations. We have recognized that the basic model did not recognize the effect of spin-induced gravity darkening on the latitudinal distribution of wind flow and consequently on disc density structure. We have included this effect and found that, although increasing S_0 from zero favours disc formation, at high S_0 the polar shift in mass flux results in decreasing disc detectability by emission or polarization. The fact that detectability (say above half of the height of the peak values of emission and polarization in Figs 6, 7, 10 and 11) covers a quite broad rotation range in S_0 , namely $S_0 \approx 0.25$ – 0.80 , is generally in good agreement with the fact that Be star rotation rates are typically estimated to occur most frequently near 0.7 (e.g. Porter 1996, and references therein; Yudin 2001), which tends to favour fast acceleration velocity laws. Overall this means that in the MTD model, the most easily observable discs are, contrary to naive expectation, not expected from the fastest rotators, but from moderate ones, as observed, though we note the comments of Townsend et al. (2004) on the effect of gravity darkening in inferring underestimated linewidth rotation rates. Clearly the whole MTD scenario

needs further work to test it thoroughly, including reconciliation of the phenomenology, numerical MHD, and analytic MHD theoretical treatments and work on further diagnostics such as X-ray emission from the MTD deceleration shocks of Be stars for comparison with *ROSAT* and other X-ray data sets.

ACKNOWLEDGMENTS

The authors acknowledge support for this work from: UK PPARC Research Grant (JCB); NASA grant TM3-4001A (JPC, JCB); and Royal Society Sino-British Fellowship Trust Award (QL), NSFC grant 10273002 (QL); RFBR grant 01-02-16858 (AK). The comments from an anonymous referee led to a significant improvement of the paper.

REFERENCES

- Bjorkman J. E., Cassinelli J. P., 1993, *ApJ*, 409, 429
 Brown J. C., McLean I. S., 1977, *A&A*, 57, 141
 Brown J. C., Carlaw V. A., Cassinelli J. P., 1989, *ApJ*, 344, 341
 Cassinelli J. P., Nordsieck K., Murison M. A., 1987, *ApJ*, 317, 290
 Cassinelli J. P., Brown J. C., Maheswaran M., Miller N. A., Telfer D. C., 2002, *ApJ*, 578, 951
 Collins G. W., 1987, in Slettebak A., Snow T. P., eds, *IAU Colloq. 92, Physics of Be Stars*, Cambridge Univ. Press, Cambridge, p. 3
 Coté J., Waters L. B. F. M., Marlborough J. M., 1996, *A&A*, 307, 184
 Dachs J., 1987, in Slettebak A., Snow T. P., eds, *IAU Colloq. 92, Physics of Be Stars*, Cambridge Univ. Press, Cambridge, p. 149
 Donati J. F., Wade G. A., Babel J., Henrichs H. F., de Jong J. A., Harries T. J., 2001, *MNRAS*, 326, 1265
 Donati J. F., Babel J., Harries T. J., Howarth I. D., Petit P., Semel M., 2002, *MNRAS*, 333, 55
 Doazan V., 1982, in Underhill A., Doazan V., eds, *NASA SP-456, B Stars with and without Emission Lines*, NASA, Washington, p. 277
 Dougherty S. M., Waters L. B. F. M., Burki G., Coté J., Cramer N., van Kerkwijk M. H., Taylor A. R., 1994, *A&A*, 290, 609
 Hanuschik R. W., 1996, *A&A*, 308, 170
 Havnes O., Goertz C. K., 1984, *A&A*, 138, 421
 Jaschek M., Groth H. G., eds. 1982, *IAU Symp. 98, Be Stars*, Reidel, Dordrecht
 Keppens R., Goedbloed J. P., 1999, *A&A*, 343, 251
 Keppens R., Goedbloed J. P., 2000, *ApJ*, 530, 1036
 Maheswaran M., 2003, *ApJ*, 592, 1156
 Maeder A., Meynet G., 2000, *A&A*, 361, 159
 Matt S., Balick B., Winglee R., Goodson A., 2000, *ApJ*, 545, 965
 Neiner C., Hubert A.-M., Fremat Y., Floquet M., Jankov S., Preuss O., Henrichs H. F., Zorec J., 2003, *A&A*, 409, 275
 Okazaki A. T., 1997, *A&A*, 318, 548
 Owocki S. P., ud-Doula A., 2003, in Balona L.A., Henrichs H.F., Medupe R., eds, *ASP Conf. Ser. 305, Magnetic Fields in O, B, and A Stars*. Astron. Soc. Pac., San Francisco, p. 350
 Owocki S. P., Cranmer S. R., Gayley K. G., 1996, *ApJ*, 472, L115
 Owocki S. P., Gayley K. G., Cranmer S. R. 1998, in Ian Howarth, ed., *ASP Conf. Ser. Vol. 131, Properties of Hot, Luminous Stars*. Astron. Soc. Pac., San Francisco, p. 237
 Porter J. M., 1996, *MNRAS*, 280, L31
 Porter J. M., Rivinius T., 2003, *PASP*, 115, 1153
 Slettebak A., 1982, *ApJS*, 50, 55
 Slettebak A., 1988, *PASP*, 100, 770
 Slettebak A., Snow T. P., eds., 1987, *IAU Colloq. 92, Physics of Be Stars*, Cambridge Univ. Press, Cambridge
 Smith M. A., Henrichs H. F., Fabregat J., eds., 2000, *ASP Conf. Ser. 214, IAU Colloq. 175, The Be Phenomenon in Early-Type Stars*. Astron. Soc. Pac., San Francisco
 Struve O., 1931, *ApJ*, 73, 94

Telfer D. C., Brown J. C., Hanuschik R., Cassinelli J. P., 2003, in Balona L.A., Henrichs H.F., Medupe R., eds, ASP Conf. Ser. 305, Magnetic Fields in O, B, and A Stars. Astron. Soc. Pac., San Francisco, p. 291
Telting J. H., 2000, in Smith M. A., Henrichs H. F., Fabregat J., eds, ASP Conf. Ser. Vol. 214, IAU Colloq. 175, The Be Phenomenon in Early-Type Stars. Astron. Soc. Pac., San Francisco, p. 422
Townsend R., Owocki S. P., Howarth I. D. 2004, MNRAS, 350, 189
ud-Doula A., Owocki S. P., 2002, ApJ, 576, 413

ud-Doula A., Owocki S. P., 2003, in Balona L.A., Henrichs H.F., Medupe R., eds, ASP Conf. Ser. 305, Magnetic Fields in O, B, and A Stars. Astron. Soc. Pac., San Francisco, p. 343
Underhill A., Doazan V., eds. 1982, NASA SP-456, B Stars with and without Emission Lines. NASA, Washington
Yudin R. V., 2001, A&A, 368, 912

This paper has been typeset from a $\text{\TeX}/\text{\LaTeX}$ file prepared by the author.